PPPL-1927

(1)

Ph. 858

PPPL-1927

UC20-F

182
9-27-82
SA

J-5569

PPPL--1927
DE82 022226

MASTER

MODE CONVERTERS FOR GENERATING THE HE11 (GAUSSIAN-LIKE) MODE FROM TE01 IN CIRCULAR WAVEGUIDE

By

J.L. Doane

SEPTEMBER 1982

PLASMA PHYSICS LABORATORY

PRINCETON UNIVERSITY
PRINCETON, NEW JERSEY

PREPARED FOR THE U.S. DEPARTMENT OF ENERGY,
UNDER CONTRACT DE-AC02-76-CHO-3073.

NOTICE

Printed in the United States of America.

Available from:

National Technical Information Service
U. S. Department of Commerce
5285 Port Royal Road
Springfield, Virginia 22151

Price: Printed Copy $ * ; Microfische $3.50

*PAGES	NTIS Selling Price
1-25	$5.00
26-50	$6.50
51-75	$8.00
76-100	$9.50
101-125	$11.00
126-150	$12.50
151-175	$14.00
176-200	$15.50
201-225	$17.00
226-250	$18.50
251-275	$20.00
276-300	$21.50
301-325	$23.00
326-350	$24.50
351-375	$26.00
376-400	$27.50
401-425	$29.00
426-450	$30.50
451-475	$32.00
476-500	$33.50
500-525	$35.00
526-550	$36.50
551-575	$38.00
576-600	$39.50

For documents over 600 pages, add $1.50 for each additional 25 page increment.

Mode Converters for Generating the HE11 (Gaussian-Like) Mode from TE01 in Circular Waveguide

J.L. Doane

Princeton University, Plasma Physics Laboratory

Princeton, New Jersey 08544

Abstract

The HE11 mode in corrugated waveguide has a field distribution very close to that of an ideal gaussian mode. Its radiation pattern is symmetric about the waveguide axis and exhibits virtually no cross polarization. This work reports measurements on mode converters to transform the TE01 mode into HE11 for electron cyclotron heating (ECH) experiments.

The first mode converter is a 28 degree bend in 1.094-inch I.D. circular waveguide which generates TM11 from TE01 with a measured efficiency of over 95% at 60 GHz. A second converter consists of a straight corrugated waveguide section of the same I.D. in which the corrugation depth increases gradually from zero to nominally a quarter wavelength. This section converts TM11 to HE11 with an efficiency of about 97%. The overall efficiency of conversion from TE01 to HE11 exceeds 91% over a measured range of 59.2 to 60.1 GHz.

I. INTRODUCTION

The transmission, polarization, and radiation of hundreds of kilowatts of millimeter wave power is presently of considerable interest for heating plasma devices at the electric cyclotron resonance frequency. Gyrotrons, which at present are the only available sources for such heating, usually generate one or more TE0N circular electric modes. Such modes are good for power transmission in long runs of straight circular waveguide since they dissipate only small amounts of power in the waveguide walls. They are, however, unpolarized and generate an undesirable conical radiation pattern from open ended waveguide. Therefore we wish to consider converting the power into a more suitable propagating mode.

The HE11 mode in corrugated waveguide is in many respects ideal for use near plasma devices. Its radiation pattern from open-ended waveguide has a narrow central beam containing 98% of the radiated power. The radiation is linearly polarized with virtually no cross polarization. Furthermore, the transmission loss in straight waveguide is about as low for HE11 as for TE01 (Clarricoats et al., 1975) and, for a given loss, corrugated bends propagating HE11 can be made smaller than those propagating TE01 (Doane, 1981). Since the field distribution of the HE11 mode inside corrugated waveguide is a close approximation to a gaussian, the HE11 will couple efficiently to a free space gaussian mode (see the review by Kogelnick and Li, 1966) which is ideal for quasi-optical propagation using mirrors inside a crowded tokamak. Such propagation will be used to generate the extraordinary mode from the inside wall of PDX (Goldman, 1982).

The superiority of the HE11 radiation pattern relative to that of TE01 is shown in Fig. 1. These patterns were calculated for 2.5-inch I.D. waveguide at 60 GHz using far-field expressions given in Thomas, 1971, suitably

normalized for unit power. The pattern for the TE11 mode from ordinary smooth circular waveguide is similar to the HE11 pattern shown in Fig. 1 with the following differences: the on-axis power is 0.8dB higher for TE11, the E-plane beam width is narrower but with sidelobes that are about 10dB higher than for HE11, and the maximum cross polarized power (in the 45°-plane) is about 20dB below the on-axis peak for the desired polarization. The radiation pattern from polarizing antennas of the Wengenroth type (Wengenroth, 1978) is more complicated since it is the result of the superposition of several waveguide modes (cf. Table IV of Hashimoto, 1976).

Figure 2 depicts the HE11 mode in a corrugated waveguide whose diameter is much greater than a wavelength and whose corrugation depth is nominally a quarter wavelength. The straightness of the field lines leads to low cross polarization, while the taper in the field distribution toward the walls leads to low sidelobes. The field varies with radius as the J_0 Bessel function, and couples efficiently at open ended waveguide to a gaussian beam with beam waist radius $w_o = 0.6435a$ (Abrams, 1972).

The HE11 mode can be generated from TE01 by the two-step process shown in Fig. 3. [If necessary, the TE01 itself can be generated from another TE0N mode present at the gyrotron output by a simple and efficient rippled-wall converter (Moeller, 1982).] First, a smooth waveguide is bent at the proper angle to convert virtually all of the TE01 power to TM11. This mode is now polarized with a polarization perpendicular to the plane of the bend, but it has higher loss and also a very undesirable radiation pattern. To convert TM11 to HE11 with low spurious mode generation, we can use a waveguide whose corrugation (slot) depth is tapered gradually from zero to nominally one-quarter wavelength.

The basic mechanisms used in these converters can be understood with reference to Fig. 4, which shows the longitudinal propagation constants β_z relative to TE01 for various important modes at 60 GHz in 1.094-inch I.D. corrugated waveguide. The case for zero slot depth corresponds to smooth waveguide, in which TM11 and TE01 have identical β_z. Constant curvature continually couples TE01 to TM11; we only have to truncate the bend at the proper angle in order to obtain TM11 from TE01. Then by gradually increasing the corrugation (slot) depth we move "adiabatically" on the curve from TM11 to HE11 without hopping to another mode. Note that the character of the HE11 mode is well established for slot depths as small as about $\lambda/8$.

Because the relative propagation constants are inversely proportional to the square of the waveguide diameter, various unwanted modes get too close for practical converters to be made in 2.5-inch I.D waveguide. The smaller I.D. was chosen to shorten the required converter length, while still maintaining relatively low loss transmission and high power handling capability. The 1.094-inch diameter is available commercially in the form of precision WC109 smooth circular waveguide. The TM11 to HE11 converter is electroformed, and an electroformed corrugated taper with fixed slot depth is used to bring the diameter back to 2.5 inches.

II. TE01-TM11 CONVERTER

In practice, the smooth TE01 to TM11 converter must be made long enough to prevent the generation of other unwanted modes while still being relatively short to minimize dissipation in the high-loss TM11 mode. To analyze the mode conversion, first consider the coupled mode equations for two modes (Rowe and Warters, 1962):

$$G_0'(z) = Kc(z)e^{\Delta\Gamma z}\, G_1(z) \ , \tag{1a}$$

$$G_1'(z) = -K^*c(z)e^{-\Delta\Gamma z}G_0(z) \ , \tag{1b}$$

where G_0 and G_1 represent the (complex) amplitudes of the two modes, and the difference in propagation constants is

$$\Delta\Gamma = \Delta\alpha + j\Delta\beta = (\alpha_0 - \alpha_1) + j(\beta_0 - \beta_1) \ . \tag{2}$$

The propagation factors $\exp(-\alpha z - j\beta z)$ have been removed so that Eqs. (1a) and (1b) relate only to mode conversion effects. The prime denotes differentiation with respect to z.

If we let G_0 and G_1 represent TE01 and TM11, respectively, then we have $\Delta\beta = 0$, and $c(z)$ represents the curvature. Furthermore, the effect of nonzero $\Delta\alpha$ is small in this case, so we can set $\Delta\Gamma = 0$. The solution of Eq. (1) when $G_0(0) = 1$ and $G_1(0) = 0$ is then very simple:

$$G_1(z) = -\frac{|K|}{K} \sin\left[|K| \int_0^z c(z)dz\right] \ . \tag{3}$$

Since the integral of the curvature in Eq. (3) is simply the total bend angle θ, we have

$$|G_1(z)|^2 = \sin^2(|K|\theta) \ . \tag{4}$$

To make $|G_1| = 1$, we then choose

$$\theta_c = \left(\frac{\pi}{2}\right)/|K| \tag{5}$$

for the total converter angle θ_c. The curvature coupling coefficient K is given in Rowe and Warters, 1962:

$$K(TE01\text{-}TM11) = j \frac{\sqrt{2}\pi a}{3.8317\lambda} , \tag{6}$$

which when combined with Eq. (5) yields

$$\theta_c = \frac{3.8317\lambda}{2\sqrt{2}\, a} . \tag{7}$$

For 2a = 1.094" and f = 60 GHz (λ = 0.2"), we find $|K|$ = 3.2 and θ_c = 28 degrees.

Other undesired modes will be generated if the 28 degree bend is too short. The most important mode coupling in the TE01 in TM11 converter is depicted in Fig. 5. Curvature couples TE01 with TM11 and TE11, and TE21 with TM11 and TE11. In the process of bending, some ellipticity is invariably produced in the waveguide which couples TE01 with TE21 and TM11 with TE11.

To predict the amount of spurious mode power leaving the TE01 to TM11 converter, generalization of Eqs. (1a) and (1b) to a set of four simultaneously coupled differential equations is required. The coupling coefficients K for these equations are listed in Table I. For curvature coupling, K is multiplied by the curvature c(z) as in Eqs. (1a) and (1b). For ellipiticity coupling, K must be multiplied by $a_2(z)$, which expresses the elliptic deformation of the cross section with nominal radius r = a:

$$r(\phi,z) = a + a_2(z) \cos 2\phi . \tag{8}$$

Here ϕ is the polar coordinate with $\phi = 0$ in the plane of the bend. The ellipticity induced by bending is such that a_2 is negative. Far above cutoff, the curvature K are proportional to af, while the ellipticity K are proportional to $a^{-3}f^{-1}$, where f is the frequency.

TABLE I.

Coupling Coefficients for Curvature and

Ellipticity in Smooth 1.094 inch I.D. Circular Waveguide at 60 GHz

Coupled Modes	Coupling Coefficient K
TE01-TM11	j 3.20
TE01-TE21	j 2.1 in^{-2}
TE01-TE11	j 3.21
TM11-TE11	j 0.7 in^{-2}
TM11-TE21	j 2.83
TE11-TE21	j 5.19

Numerical integration of the coupled mode equations shows that at 60 GHz for a bend in 1.094-inch (WC109) waveguide, constant curvature produces less spurious mode power than a variable c(z). The effect of ellipticity is shown in Fig. 6. The ellipticity $a_2(z)$ is assumed to be constant throughout the bend just as the curvature is. For the shorter bend, ellipticity increases the TE21 level (Fig. 6a). For the longer bend (Fig. 6b), ellipticity decreases the level of TE21 from its value at zero ellipticity, which is already quite low. The power in TE11 is reduced by about a factor of 2 from Fig. 6a to Fig 6b. These expectations are in accord with the measured data, which is described next.

A view of the longer TE01 to TM11 converter is shown in Fig. 7. A 57-inch piece of straight WC109 waveguide was annealed in a vacuum furnace and then was bent against a smooth form inside the aluminum frame shown. The form was machined so as to produce a 28-degree bend with constant radius of curvature over a 48-inch arc length. Steel pins pressed into precisely located holes then prevent the waveguide from moving outward again. The spacing between top and bottom plates is just slightly larger than the WC109 O.D. in order to suppress the ellipticity caused by bending. This bending frame is similar to one reported earlier that was used to bend a section of dielectric-lined waveguide to make a low loss bend (Kindermann, 1965).

A TE01 launcher-receiver pair supplied by C. Moeller of General Atomic Co., San Diego, California, was used to measure the total TE01 insertion loss through two back-to-back TE01 to TM11 converters. The insertion loss from 59.2 to 60.1 GHz oscillated within the limits of 0.3 and 0.5 dB. Taking into account the possible in-phase and out-of-phase addition of the spurious modes generated in each converter, this is consistent with an ohmic loss of 0.15dB ($\sim$ 3%) and spurious mode loss of about 0.05dB ($\sim$ 1%) per converter. This ohmic loss in turn is consistent with a theoretical TM11 ohmic loss of 0.21 dB/meter in ideal WC109 waveguide, since the total converter length is 1.45 meter (57"), and from (4) the average ohmic loss over the bend should be one-half of the TM11 loss.

The above estimate of spurious mode loss is also consistent with the direct measurements. Near 60 GHz the amount of TE01 received at the converter output varied between 0.1 to 0.3% of the input power, whereas the output TE11 power (as measured by a nonlinear taper and circular-to-rectangular TE11 to TE10 transducer) varied between 0.3 and 0.5% of the TE01 input. These measurements agree with Fig. 6b at the expected ellipticity of 2-3 mils (.002-.003 inch).

For comparison, the directly measured TE01 and TE11 levels at the output of the shorter converter with a 36 inch bend length varied between 0.2 and 0.4% and 0.7 to 1.0%, respectively, of the input TE01 power. Again, the measurements are in close agreement with Fig. 6a at an expected ellipticity of 4-6 mils (the spacing between the converter top and bottom plates was somewhat larger than for the longer converter).

The only way to measure the spurious TE21 mode power was through radiation pattern measurements using the equipment pictured in Fig. 8. Just as for the direct measurements described above, the 60 GHz power was produced by a gunn oscillator externally modulated at 1 kHz and detected by a millimeter detector and an SWR meter responding to 1 kHz. The measured E-plane pattern is superimposed on the ideal far-field TM11 radiation pattern in Fig. 9. The right peak in the measured 60 GHz pattern was adjusted to coincide with the theoretical peak. The noise level in the measurements is about 26dB below that peak.

The presence of cross polarized energy indicates TE01 or TE21, since TM11 ideally radiates no cross polarized component in the E-plane patterns. Cross polarized power was detected between 8 and 22 degrees away from the axis and peaked at a level 22-23 dB below the main peak in Fig. 9. Comparison with theoretical TE01 and TE21 patterns (which are almost identical) shows that the TE01/TE21 power at the output of the longer converter is about 25dB below TM11, or about 0.3% of the input TE01 power. Comparison with the directly measured TE01 power shows that the TE21 power cannot be much larger than the TE01 power, in agreement with Fig. 6b. For the short converter, on the other hand, the cross polarized radiation indicated that the TE01/TE21 power was about 3% of the TE01 input. This value is much larger than the directly measured TE01; hence we conclude that the TE21 power was about 3%, again in good agreement with Fig. 6a for the expected 4-6 mil ellipticity.

The fill-in of the radiation pattern on the axis (0 degrees) is due to TE11 and also to residual near-field contributions. The peak in the theoretical TE11 pattern is 4 dB above the TM11 peaks; the measured fill-in (Fig. 9) which is 18 dB below the TM11 peaks thus shows that TE11 must be at least 22 dB below the output TM11 level. This level of TE11 is close to the directly measured value (see above).

III. TM11 - HE11 CONVERTER

Conversion of TE11 to HE11 and TM11 in a corrugated circular waveguide with slowly varying corrugation slot depth has been investigated theoretically (Kerzhentseva, 1971) and experimentally (Thomas, 1972). The measurements in Thomas, 1972, performed at a relatively small waveguide diameter to wavelength ratio, indicated empirically that the conversion efficiency improved with the length of the converter. In our case the waveguide diameter 2a is much larger than a wavelength, and we must determine the converter length and slot depth variation for acceptable conversion efficiency.

Unwanted mode hopping in a TM11 to HE11 converter is associated primarily with the nearby TE11 to EH11 branch (see Fig. 4). The varying slot depth D only couples mode branches with the same first index (Dragone, 1977) so that TE21 and TM21, for example, are not a problem. The coupling can be described by equations similar to (1):

$$G_1'(z) = c(D)\,\frac{dD}{dz}\,\exp\left(j\int_0^z \Delta\beta\,dz\right)\,G_2(z) \quad , \tag{9a}$$

$$G_2'(z) = -c(D)\,\frac{dD}{dz}\,\exp\left(-j\int_0^z \Delta\beta\,dz\right)\,G_1(z) \quad , \tag{9b}$$

where G_1 represents the TM11 to HE11 mode branch, and G_2 represents the TE11 to EH11 branch. The exponential factors are more complicated than in (1), because the difference in propagation contants $\Delta\beta = \beta_1 - \beta_2$ changes with D. The coupling coefficients c(D) are easily obtained from Eqs. (141) and (142) of Dragone, 1977, by a change of variables. To calculate c(D), the propagation constants β_1 and β_2 must first be calculated from Eq. (20) of Dragone, 1977. These are most easily found by following the Bessel function roots as D is gradually increased from D = 0 and using Newton-Raphson techniques. The root for TE11-EH11 becomes imaginary for a slot depth greater than about 0.1 $\lambda/4$, representing the fact that this mode branch becomes a surface wave. Eventually the attenuation α for this branch becomes quite large as D increases and the field becomes more tightly bound to the walls. We can neglect this attenuation in (9), however, because the coupling c(D) becomes very small at these D (Fig. 10).

To design the converter, we require that the coupling in Eq. (9) be a constant K_c, and hence $\Delta D = K_c \Delta z / c(D)$. In this way we increase the slot depth most slowly near the beginning ($D \gtrsim 0$) where the coupling is strongest. The constant K_c is determined iteratively by the requirement that the slot depth must reach the desired value at the end of the converter. In generating the D(z) profile, a small correction was made for the reduction in X_s caused by the finite width between slots; that is, the mechanical slot depth was increased relative to the desired electrical slot depth profile.

To prevent the power in EH11 or EH21 surface waves from causing breakdown, we truncated the converter at D = 0.5 ($\lambda/8$ slot depth). EH21 can result from residual TE21 leaving the TE01-TM11 converter (see Fig. 4); EH11 can come from residual TE11 generated in that converter or from mode hopping in the TM11-HE11 converter. For larger D than 0.5, the peak electric field

for a given power carried by EH11 or EH21 increases as the normalized surface reactance $X_s = \tan(0.5\pi D)$. At D = 0.5, the theoretical power-handling capability in EH11 or EH21 for a given breakdown field is 4% of that which can be carried by TE01. The residual TE11 and TE21 from the TE01-TM11 converter is low (Fig. 6b), and the power coupled into EH11 is small for reasonable TM11-HE11 converter lengths (Fig. 11). Hence breakdown should not be a problem. The price paid is only that the peak in the radiation pattern main lobe for HE11 is reduced by 0.12dB at D = 0.5 as compared with D = 1.0 ($\lambda/4$ slot depth).

The corrugation period was made $\lambda/8$ = .025", which is considerably smaller than $\lambda/2$, in order to avoid higher order space harmonics. The guide wavelength $2\pi/\beta_z$ can become quite small for EH11 or EH21 at large D (about $\lambda/\sqrt{2}$ at D = 0.5 and in general $\sim \lambda/\sqrt{1 + X_s^2}$). The slot width is nominally half the corrugation period.

The actual converter tested at 60 GHz is pictured in Fig. 12. Its overall length is 15 inches. Even though the expected level of undesired EH11 and EH21 surface waves is quite low, especially with the longer TE01-TM11 converter, the TM11-HE11 converters were electroformed of nickel rather than copper in order to increase the attenuation of any residual surface wave power.

The measured output H-plane pattern of the TM11-HE11 converter is shown in Fig. 12 superimposed on the ideal pattern. The input to the TM11-HE11 converter was fed from the TE01-TM11 converter of Figs. 7 and 9. The measured E-plane pattern was virtually identical to the H-plane pattern, as expected theoretically. We conclude that a highly pure HE11 mode was generated.

The measured insertion loss of the TM11-HE11 converters was about 0.12dB per converter. This loss was determined by first inserting and then removing

two back-to-back TM11-HE11 converters between two TE01-TM11 converters. Comparison with Fig. 11 suggests that there was little added ohmic loss in the desired mode due to the higher nickel wall resistivity. Original insertion loss measurements made soon after cleaning were about 1.5dB higher, presumably due to the presence of moisture in the corrugations.

The overall TE01 to HE11 conversion efficiency was measured between 59.2 and 60.1 GHz. The measured insertion loss from TE01 to HE11 and back through a pair of TE01-TM11 converters and a pair of TM11-HE11 converters was 0.8dB or less accross this band. We conclude that the loss from TE01 to HE11 was less than 0.4dB and hence that the conversion efficiency was better than 91%.

ACKNOWLEDGMENT

The author is happy to acknowledge many helpful discussions with H. Hsuan, M. Goldman, and N. Bowen, the assistance of George Ioannidis and Werner Schiedt in making the TE01-TM11 converter frame, and the assistance of Ed Hall in annealing and bending the waveguide. The TM11-HE11 converter was electroformed by the A.J. Tuck Co., Brookfield, Connecticut. This work was supported by the U.S. Department of Energy Contact No. DE-AC02-76-CHO-3073.

REFERENCES

Abrams, R.L. (1972). "Coupling Losses in Hollow Waveguide Laser Resonators," IEEE J. Quant. Electron, Vol. QE-8, pp 838-843.

Clarricoats, P.J.B., Olver, A.D., and Chong, S.L. (1975). "Attenuation in corrugated circular waveguides, Parts I and II: Theory and Experiment," Proc. IEE, Vol. 122, pp. 1173-1183.

Doane, J.L. (1981), unpublished work.

Dragone, C. (1977). "Reflection, Transmission, and Mode Conversion in a Corrugated Feed," Bell System Tech. J., Vol. 56, pp. 835-867.

Goldman, M.A. (1982), private communication.

Hashimoto, Junio (1976). "Circular TE0N Mode Filters for Guided Millimeter-Wave Transmission," IEEE Trans. Microwave Theory Tech., Vol. MTT-24, pp. 25-31.

Kerzhentseva, N.P. (1971). "Conversion of Wave Modes in a Waveguide with Slowly Varying Impedance of the Walls," Radio Engineering and Electronic Physics, Vol. 16, pp. 24-31.

Kindermann, H.P. (1965). "Optimierte H_{01}-Krümmer mit dieklektrischer Schicht," A.E.Ü, Vol. 19, pp. 699-701.

Kogelnik, H. and Li, T. (1966). "Laser Beams and Resonators," Appl. Opt., Vol. 5, pp. 1550-1567.

Moeller, C. (1982). "Mode Converters used in the Doublet III ECH Microwave System," Second U.S. Gyrotron Conference, Washington, D.C., June 21-23, 1982.

Rowe, H.E. and Warters, W.D. (1962). "Transmission in Multimode Waveguide with Random Imperfections," Bell System Tech. J., Vol. 41, pp. 1031-1170.

Thomas, B. MacA. (1971). "Theoretical Performance of Prime-Focus Paraboloids Using Cylindrical Hybrid Mode Feeds," Proc. IEE, Vol. 118, pp. 1539-1549.

Thomas, B. MacA. (1972). "Mode Conversion Using Circumferentially Corrugated Cylindrical Waveguide," Electron Lett., Vol. 8, pp. 394-396.

Wengenroth, R.D. (1978). "A Mode Transducing Antenna," IEEE Trans. Microwave Theory Tech., Vol. MTT-26, pp. 332-334.

FIGURE CAPTIONS

Fig. 1 Ideal radiation patterns for open ended 2.5-inch I.D. circular waveguide carrying the TE01 or HE11 mode at 60 GHz. Power received in a small probing antenna with 10 dB gain located 40 inches from aperture of waveguide, which is transmitting power at a 0dB reference level.

Fig. 2 The HE11 mode in waveguide with $a/\lambda >> 1$. The radial field distribution is close to gaussian.

Fig. 3 Generation of HE11 from TE01. TM11 and HE11 are polarized perpendicular to the plane of the bend.

Fig. 4 Propagation constants relative to TE01 in 1.094-inch I.D. corrugated circular waveguide as a function of slot depth at 60 GHz.

Fig. 5 Important modes in the TE01 to TM11 converter. Curvature coupling is represented by arrows around the perimeter of the diamond; ellipticity coupling by arrows across the diamond.

Fig. 6 Theoretical spurious mode power at the output of 1.094 - inch I.D. constant curvature TE01 to TM11 converters at 60 GHz as a function of ellipticity induced by bending.

a) Bend arc length = 36 inches

b) Bend arc length = 48 inches

Fig. 7 TE01 to TM11 converter, 48-inch bend length, 57-inch overall length.

Fig. 8 Experimental apparatus used to measure radiation patterns.

Fig. 9 Measured E-plane radiation patterns of 57-inch TE01 to TM11 converter (indicated by points X) superimposed on ideal TM11 pattern. Separation of transmitting and receiving apertures is 20".

Fig. 10 Coupling coefficient for branch hopping from TM11-HE11 to TE11-EH11 due to changing slot depth at 60 GHz in 1.094-inch I.D. waveguide.

Fig. 11 Theoretical mode conversion loss versus length of a TM11 to HE11 converter in 1.094-inch I.D. corrugated waveguide at 60 GHz. The slot depth profile is assumed to give constant coupling and is truncated at D = 0.5 ($\lambda/8$ slot depth).

Fig. 12 TM11-HE11 converter, 15-inch overall length.

Fig. 13 Measured H-plane radiation pattern at the output of the HE11 converter (indicated by points X) superimposed on ideal HE11 pattern for 1.094-inch I.D. Converter is fed by the TE01 to TM11 converter of Fig. 7; separation of transmitting and receiving apertures is 20".

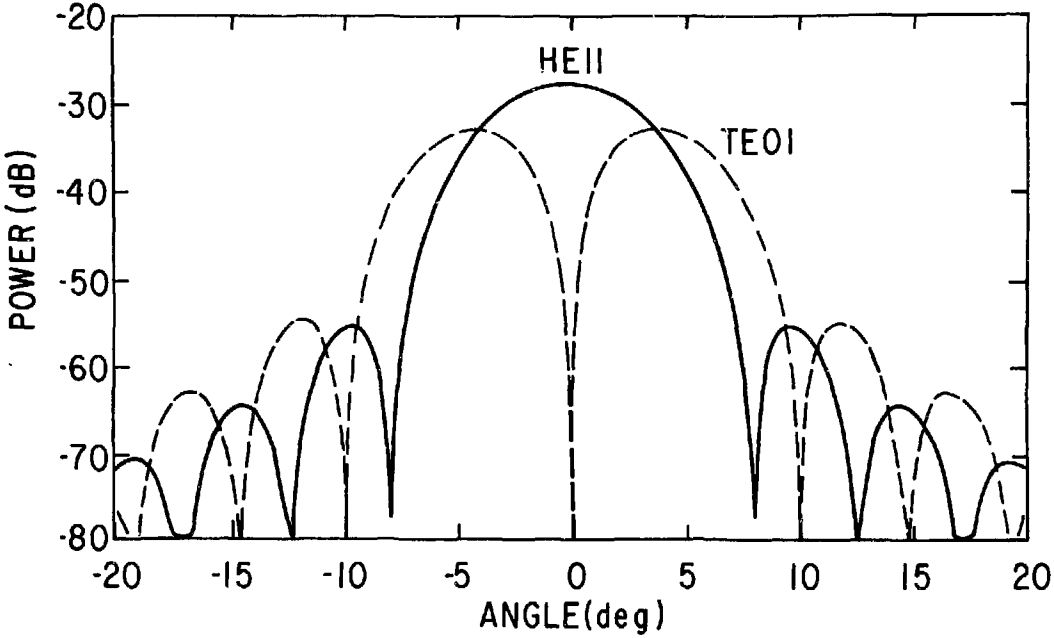
HE11
TE01
POWER (dB)
-20
-30
-40
-50
-60
-70
-80
-20
-15
-10
-5
0
5
10
15
20
ANGLE(deg)

Fig. 1

#82E0088

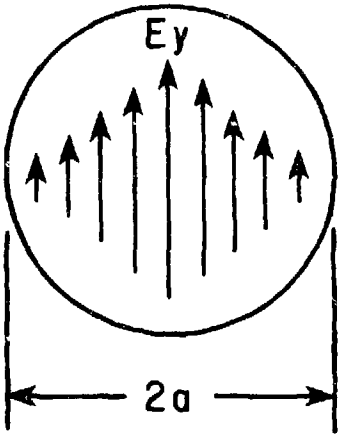

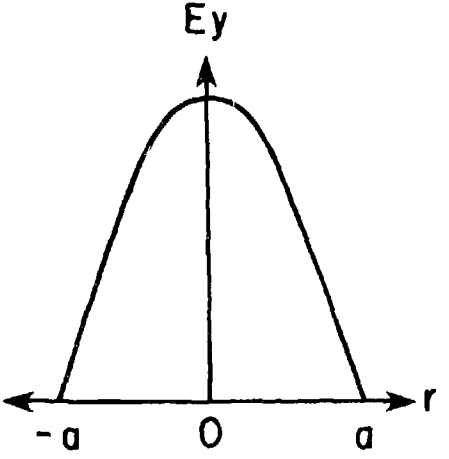

Fig. 2

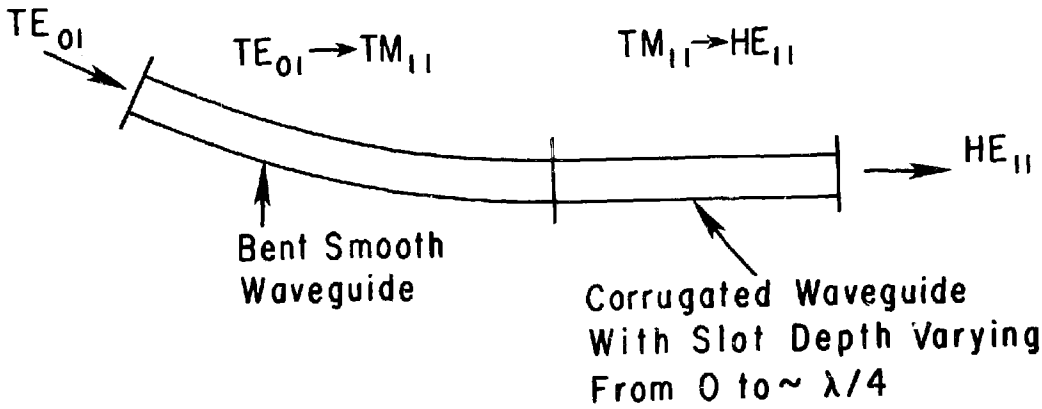
TE01
TE01→TM11
TM11→HE11
HE11
Bent Smooth
Waveguide
Corrugated Waveguide
With Slot Depth Varying
From 0 to~ λ/4

Fig. 3

#82E0094

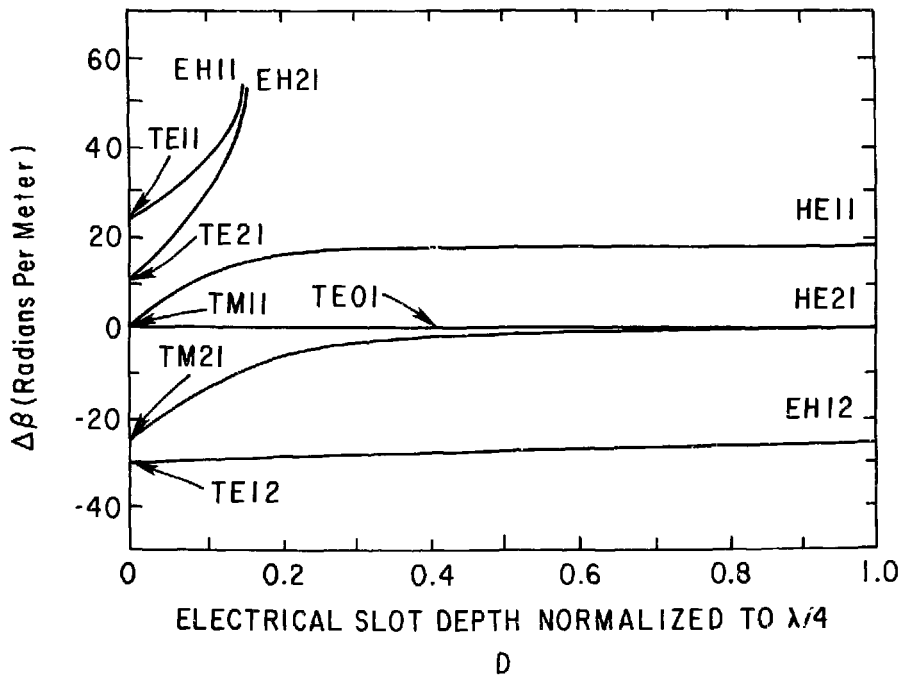

Fig. 4

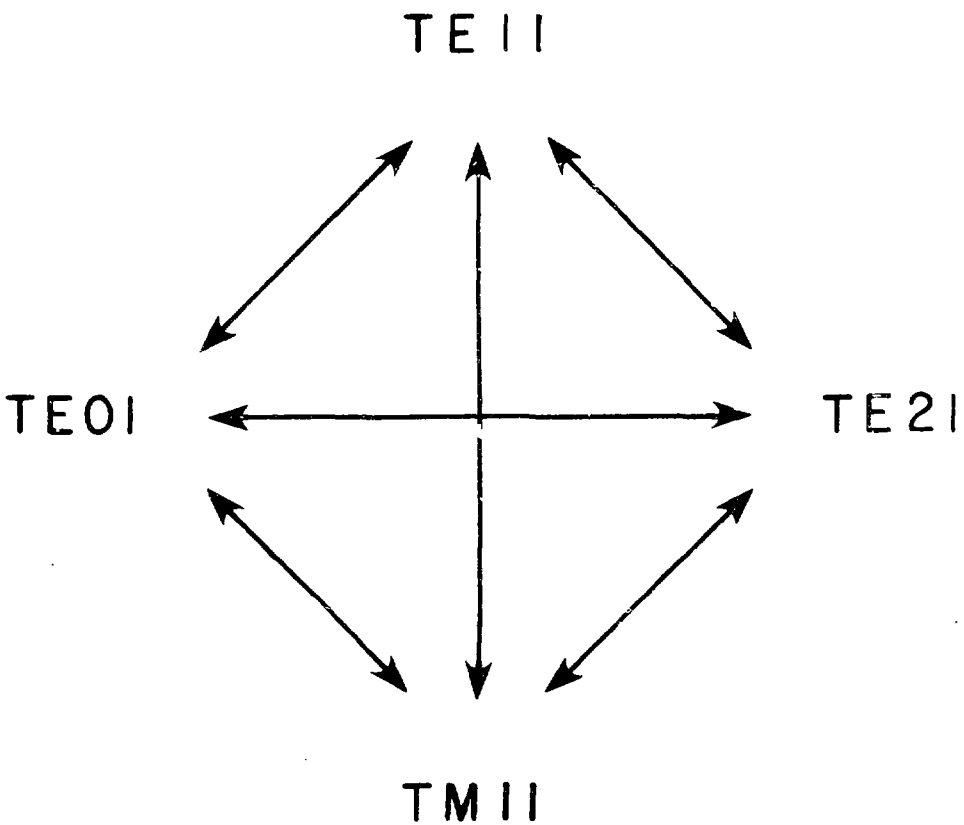

Fig. 5

#82E0089

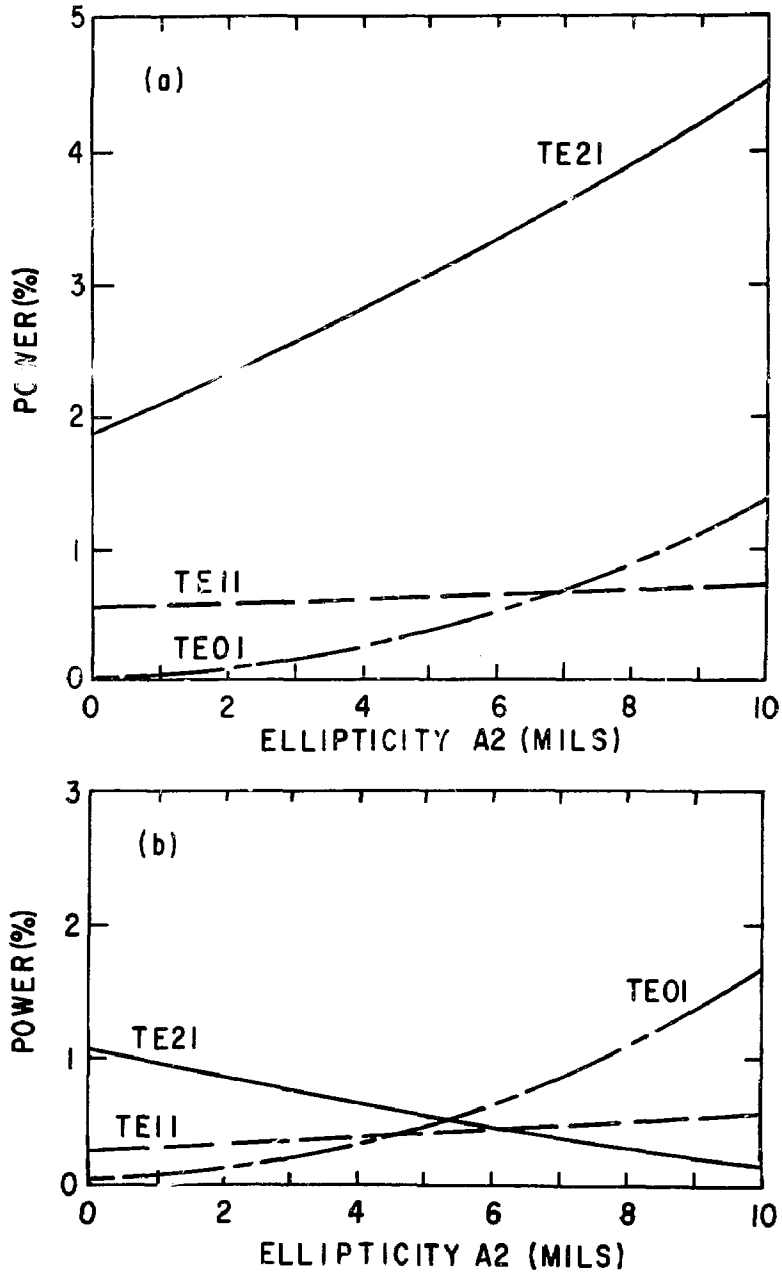

Fig. 6

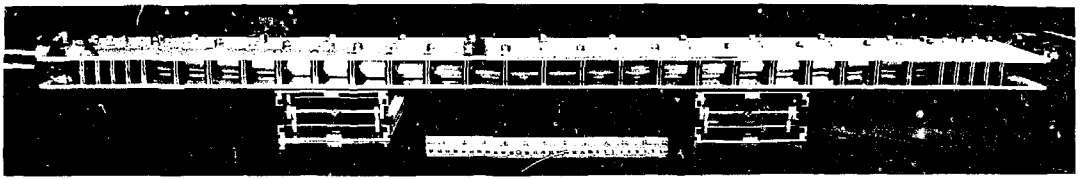

Fig.

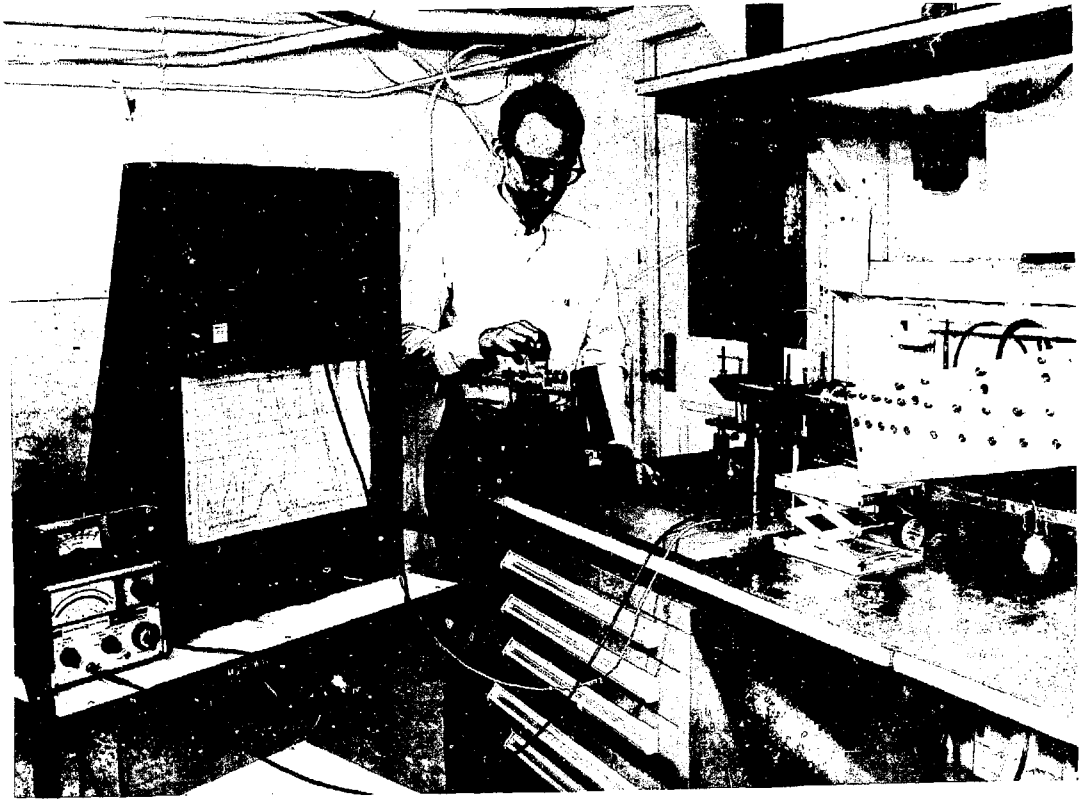

Fig. 8

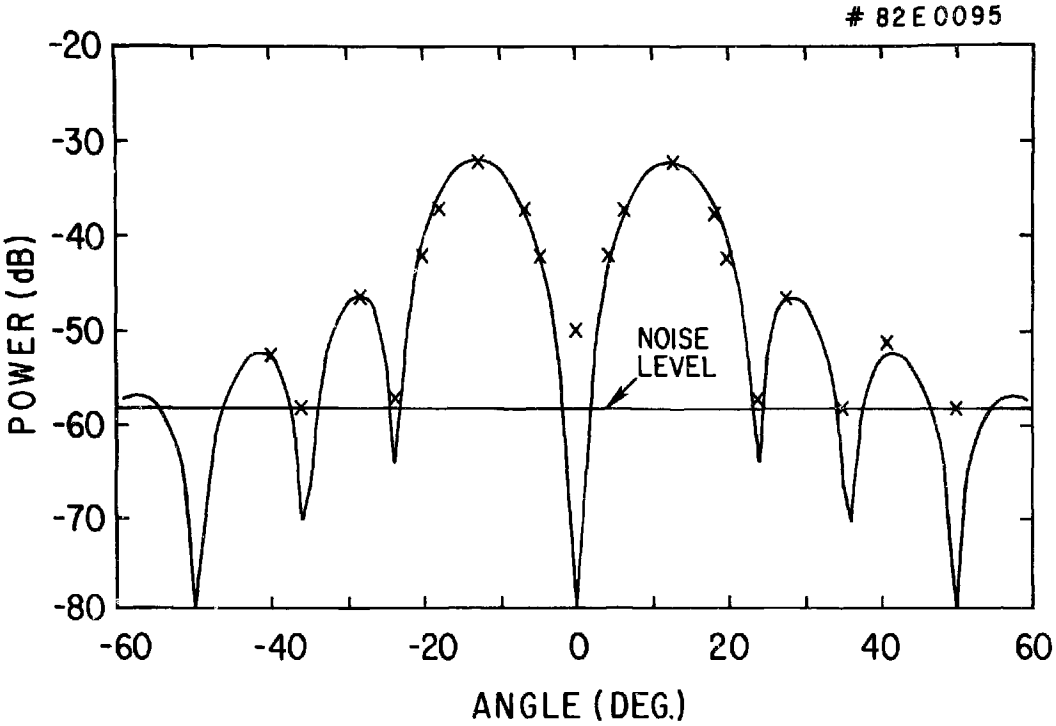
82E0095
-20
-30
-40
-50
-60
-70
-80
POWER (dB)
NOISE
LEVEL
-60
-40
-20
0
20
40
60
ANGLE (DEG.)

Fig. 9

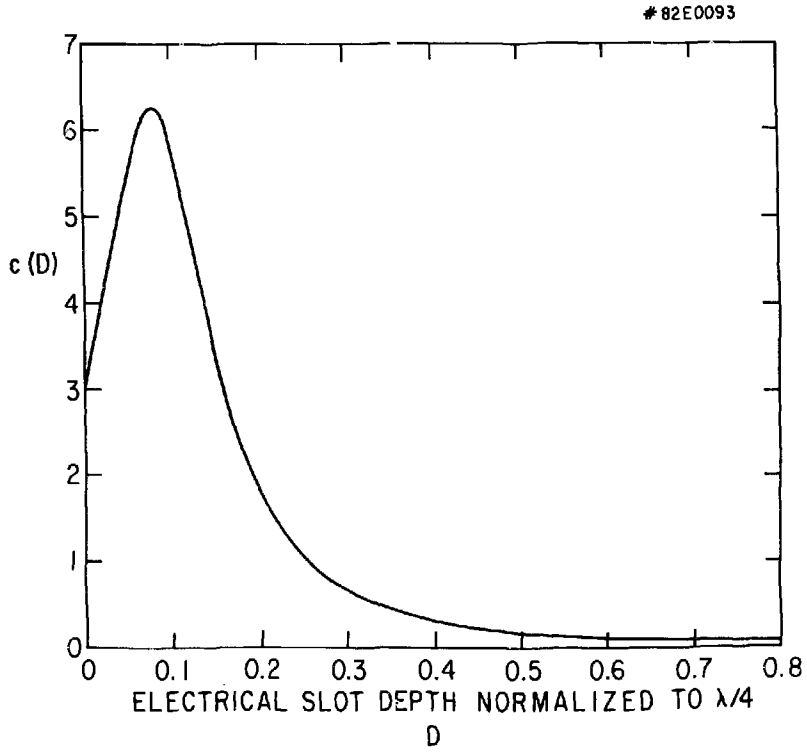
#82E0093
7
6
5
4
3
2
1
0
c (D)
0
0.1
0.2
0.3
0.4
0.5
0.6
0.7
0.8
ELECTRICAL SLOT DEPTH NORMALIZED TO λ/4
D

Fig. 10

#82E0091

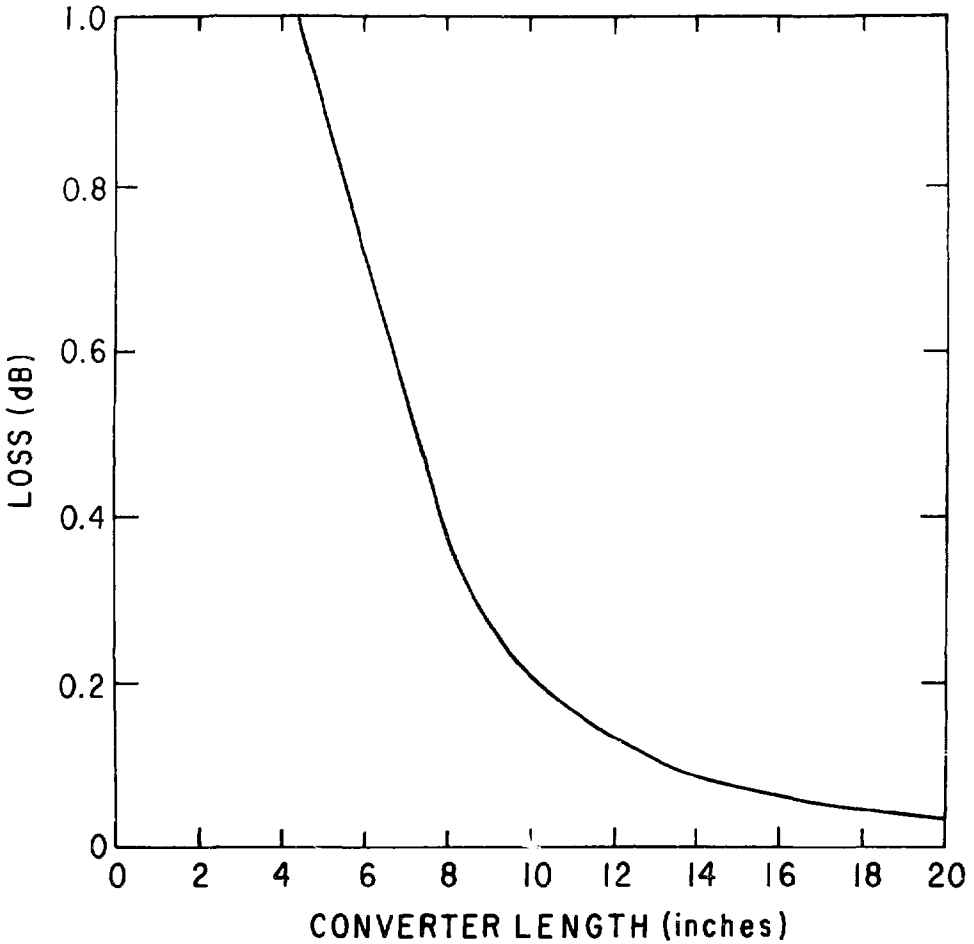

Fig. 11

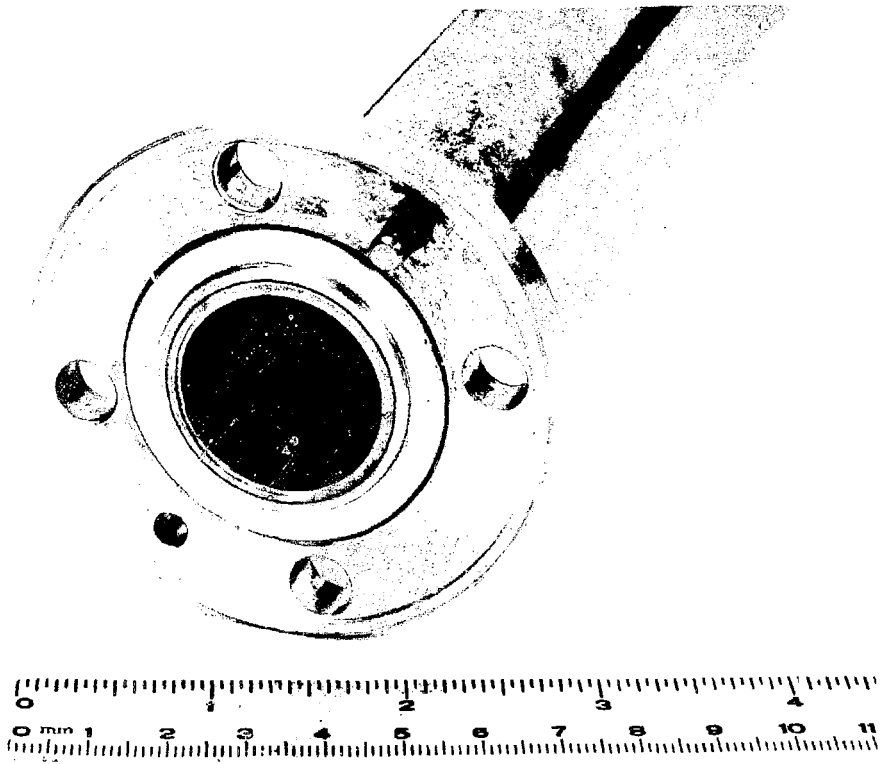

Fig. 12

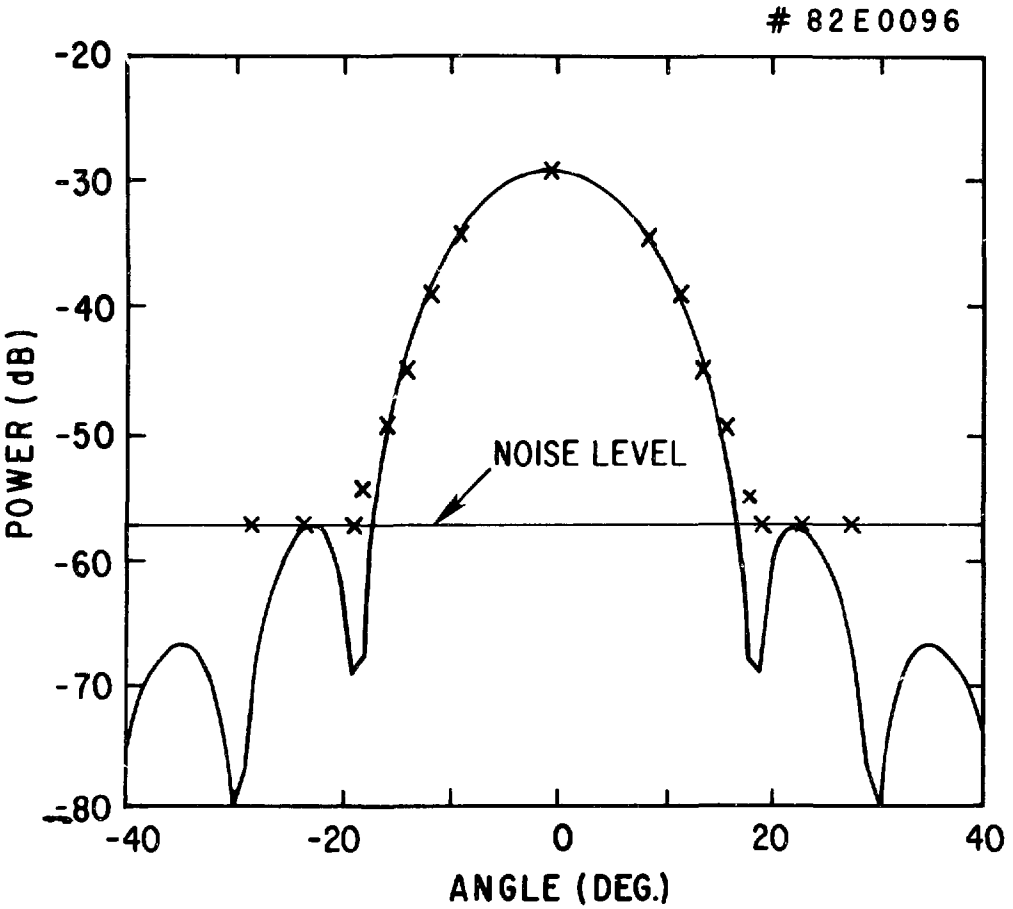
82E0096
-20
-30
-40
-50
-60
-70
-80
POWER (dB)
NOISE LEVEL
-40
-20
0
20
40
ANGLE (DEG.)

Fig. 13